Acute and Chronic Ventricular-Arterial Coupling in Systole and Diastole
Insights From an Elderly Hypertensive Model

Brian P. Shapiro, Carolyn S.P. Lam, Jeetendra B. Patel, Selma F. Mohammed, Martina Kruger,
Donna M. Meyer, Wolfgang A. Linke, Margaret M. Redfield

Abstract—Aging and hypertension lead to arterial remodeling and tandem increases in arterial (Ea) and ventricular (LV) systolic stiffness (ventricular-arterial [VA] coupling). Age and hypertension also predispose to heart failure with normal ejection fraction (HFnlEF), where symptoms during hypertensive urgencies or exercise are common. We hypothesized that: (1) chronic VA coupling also occurs in diastole, (2) acute changes in Ea are coupled with shifts in the diastolic and systolic pressure-volume relationships (PVR), and (3) diastolic VA coupling reflects changes in LV diastolic stiffness rather than external forces or relaxation. Old chronically hypertensive (OHT, n=8) and young normal (YNL, n=7) dogs underwent assessment of PVR (caval occlusion) and of aortic pressure, dimension, and flow, at baseline and during changes in afterload and preload. Concomitant changes in the slope/position of PVR were accounted for by calculating systolic (ESV_{200}) and diastolic (EDV_{20}) volumes at common pressures (capacitance). OHT displayed marked vascular remodeling. Indices reflecting the pulsatile component of Ea (aortic stiffness and systemic arterial compliance) were more impaired in OHT at any distending pressure. In both groups, acute increases in Ea were associated with decreases in ESV_{200} and EDV_{20}. However, at any load, OHT had lower ESV_{200} and EDV_{20}, associated with LV remodeling and myocardial endothelin activation. Acute changes in EDV_{20} were not mediated by changes in relaxation or external forces. These observations provide insight into the mechanisms whereby arterial remodeling and acute and chronic VA coupling in both systole and diastole may predispose to and interact with increases in load to cause HFnlEF. (*Hypertension*. 2007;50:503-511.)

Key Words: hypertension, experimental ■ hypertension, elderly ■ ventricular function, left ■ diastole ■ heart failure ■ vasculature ■ endothelin

Systemic hypertension and advanced age are the dominant risk factors for heart failure (HF) with a normal ejection fraction (HFnlEF).[1] Both age and chronic hypertension predispose to vascular remodeling with increases in vascular stiffness, the speed and magnitude of reflected waves, and, thus, late systolic ventricular (LV) load.[2] These chronic vascular changes are coupled to increases in LV systolic stiffness (Ees).[3,4] Although chronic systolic ventricular-arterial (VA) coupling serves to maintain stroke work (SW), it also predisposes to adverse effects including increased sensitivity to changes in volume and limited systolic reserve.[3,4] These adverse effects have been postulated to play a role in the pathophysiology of HFnlEF.[5]

Coupling of ventricular and vascular function during acute changes in arterial load is also important to consider as a significant subgroup of elderly patients with HFnlEF present with pulmonary edema during a hypertensive urgency or with exertional symptoms associated with an exaggerated hypertensive response to exercise.[6,7] The specific mechanisms mediating the association between transient increases in blood pressure and increases in filling pressures and symptoms in HFnlEF are not fully defined. Isolated increases in preload may lead to concomitant increases in blood pressure, LV volume, and filling pressures. However, Gandhi et al studied HFnlEF patients during and after hypertensive pulmonary edema and found that LV diastolic volume was not increased and ejection fraction (EF) was not decreased during versus after pulmonary edema.[6] Further, studies in patients with exercise intolerance and hypertensive responses to exercise do not demonstrate consistent increases in LV volume or decreases in EF.[8] These findings suggest transient afterload induced shifts in both the systolic (ESPVR) and diastolic (EDPVR) pressure-volume relationship (PVR). Whereas acute enhancement of systolic performance with

increases in afterload is well described,[9–13] acute changes in the EDPVR with increases in afterload have been variably ascribed to an effect of external forces, impairment in relaxation, or acute changes in diastolic stiffness or distensibility.[5,6,14,15]

The objective of this study was to gain insight into the mechanisms underlying the association between vascular and ventricular function in HFnlEF and, in particular, during transient changes in blood pressure. We hypothesized that: (1) as in systole, chronic VA coupling also occurs in diastole with shifts in the slope/position of the EDPVR with chronic increases in Ea, (2) acute changes in Ea are coupled with changes in both diastolic and systolic PVR (acute VA coupling), and (3) both acute and chronic diastolic VA coupling reflects changes in LV diastolic stiffness or distensibility rather than effects of external forces or relaxation. Thus, vascular structure and function and their relationship to ventricular function were assessed in normal young dogs (YNL) and elderly dogs with chronic hypertension (OHT). As vascular (and ventricular) properties themselves may vary with changes in blood pressure, the analysis focused on the relationship between load and vascular function and ventricular systolic and diastolic performance in each group. Finally, we sought to determine whether changes in ventricular structure and function were associated with local activation of prohypertrophic/profibrotic factors such as endothelin, transforming growth factor (TGF)-$\beta1$, or angiotensin II.

Methods

The Mayo Institutional Animal Care and Use Committee approved all experimental procedures used in the study, which included euthanasia consistent with the Panel on Euthanasia of the American Veterinary Medical Association guidelines. Please see http://hyper.ahajournals.org for the online supplement for additional details regarding methods.

Experimental Hypertension

Old mongrel dogs (n=8, age 8 to 12 years) were made hypertensive by bilateral renal wrapping (OHT) as previously described.[16] An indwelling aortic catheter connected to a subcutaneous access port was placed for weekly conscious blood pressure (BP) measurements. Dogs were followed for 8 weeks after wrapping. Young dogs (n=7, age ≈1 year) were used as controls (YNL) and did not undergo chronic BP measurements. The animals used in this study were provided from a Class A supplier, Twin Valley in Spring Green, Wisc.

Acute Hemodynamic Study

Dogs were anesthetized with intravenous (IV) fentanyl (0.25 mg/kg bolus followed by 0.18 mg/kg per hour) and midazolam (0.75 mg/kg bolus followed by 0.59 mg/kg per hour), intubated, and ventilated with supplemental oxygen as previously described.[17] Animals were instrumented with an ascending aortic micromanometer, volumetric flow probe and piezoelectric crystals, a LV conductance catheter, a pneumatic inferior vena cava (IVC) occluder, and a left atrial pacing wire. The conductance signal was converted to a left ventricular volume by the formula: $V=(1/\alpha)\cdot(rho\cdot L^2)\cdot([G-G_P])$ where α=slope factor, rho=specific resistivity of blood measured from a 5-mL blood sample, L=distance between electrodes, G=total conductance, and G_P=parallel conductance. G_P was determined via the hypertonic saline method and α was derived from the aortic flow probe stroke volume (SV). Dogs received propanolol (2 mg/kg IV) and atropine (1.0 mg IV) and were atrial paced at 10 to 20 bpm above sinus rate. Steady-state data and data during acute IVC occlusion

were obtained at baseline (BL), during phenylephrine infusion to achieve LV peak systolic pressure of 150 to 175 mm Hg (PE-1) and then 200 to 250 mm Hg (PE-2), after recovery from phenylephrine (BL-2) and after acute volume expansion (VE) with dextran (500 mL over 30 minutes). The heart and aorta were harvested.

Hemodynamic Analysis

The end-systolic pressure (ESP) volume (ESV) relationship (ESPVR) was defined as ESP=Ees (ESV-V_0), and the end-diastolic pressure (EDP) volume (EDV) relationship (EDPVR) as EDP=$\alpha e^{(\beta EDV)}$. Ees was also normalized to myocardial volume (Ees·myocardial volume). Recognizing the covariance between Ees and V_0 and constraints imposed by the nonlinearity of the ESPVR and the limited pressure range over which assessment of the ESPVR occurs in vivo, afterload enhancement of myocardial performance may manifest as increases in the slope (increased E_{es}) or a parallel leftward shift of the ESPVR. Thus, the ESV at an ESP of 200 mm Hg (ESV_{200}=(200/Ees)+Vo)[18] was calculated to reflect systolic capacitance, inversely related to systolic stiffness. This variable would be similarly decreased by an increase in Ees or a leftward shift of the measured ESPVR. To account for the exponential configuration of the EDPVR with covariance between α and β where both describe the shape and position of the EDPVR, diastolic capacitance was characterized as the EDV at an EDP of 20 mm Hg (EDV_{20}=[ln(20/α)]/β).[18] Analogous to the ESP_{200}, the EDV_{20} would be similarly reduced by an increase in the slope or a parallel upward/leftward shift in the position of the EDPVR. As the α and β used to calculate EDV_{20} were derived from the EDPVR defined by acute preload reduction, a decrease in the EDV_{20} as defined above was not confounded by potential effects of external forces. The kinetics of LV relaxation and the potential impact on LV filling pressures were characterized by determining what portion of diastole was needed for relaxation to be complete. Relaxation time was calculated as 3.5·the time constant of isovolumic relaxation (τ), assuming a zero asymptote or nonzero asymptote and expressed as relaxation time/diastolic period.[19,20]

As the characteristics of the arterial wall vary with distending pressure and geometry, comparison of vascular properties between hypertensive and nonhypertensive cohorts will reflect not only differences in the intrinsic properties of the vessel wall but also the effects of distending pressure and vessel geometry. Accordingly, the relationship between arterial properties and pressure should be defined and comparisons between groups adjusted for differences in distending pressure.[21] Thus, we assessed vascular function over a range of distending pressures produced by peripheral vasoconstriction and volume expansion in YNL and OHT. As aortic stiffness increases and total arterial compliance decreases with increasing distending pressure, the relationship between these variables and mean arterial pressure was compared between groups. To further demonstrate the impact of factors influencing the pulsatile (aortic elastic modulus and arterial compliance) components of load on total load, we examined the relationship between peripheral vasoconstriction (systemic vascular resistance, SVR) and total load (Ea) between groups. SVR was calculated as mean arterial pressure (MAP)/cardiac output and expressed as dyne·sec·cm^{-5}. Ea was calculated as ESP/SV. Aortic stiffness was quantified by Peterson elastic modulus ((Ps-Pd)·Dd)/(Ds−Dd) expressed as ·10^6 dyne/cm^2 where Ps and Pd are aortic systolic and diastolic pressures and Ds and Dd are aortic systolic and diastolic dimensions.[22] Systemic arterial compliance (SAC) was calculated using the method of Liu et al where SAC is assessed during diastole as $\int$AoP (from P_{DN} to Pd) /SVR (P_{DN}−Pd) where P_{DN} is aortic P at the dicrotic notch and Pd is aortic pressure at end-diastole.[23]

Histological and Biochemical Analysis

Quantitative histomorphometry was performed on picrosirus red or LELVG stained tissue samples for calculation of collagen volume fraction (CVF), elastin density, and aortic wall thickness. LV and aortic total collagen content and collagen solubility (24-hour pepsin digestion, 1 mg/mL) were quantified using the hydroxyproline assay.[24] Myocardial atrial (ANP) and brain (BNP) natriuretic peptide, angiotensin II (AII), and endothelin-1 (ET-1) were measured by
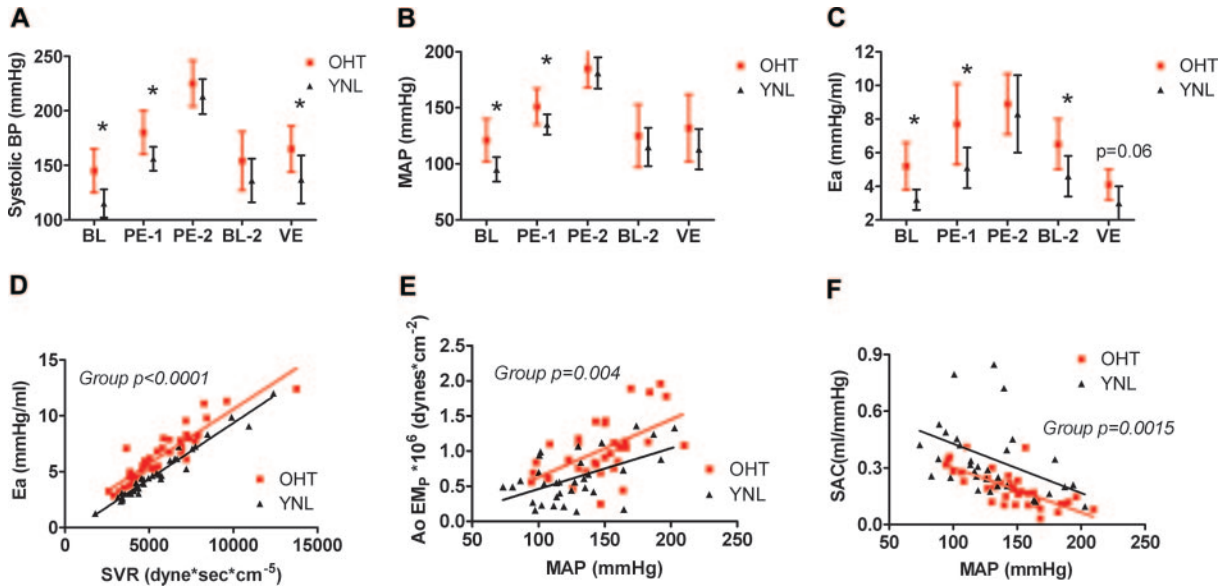
Figure 1. Systolic blood pressure (BP; A), mean arterial pressure (MAP; B), and effective arterial elastance (Ea; C) in OHT (red) and YNL (black) dogs at baseline (BL), phenylephrine-1 (PE-1), phenylephrine-2 (PE-2), baseline-2 (BL-2), and volume expansion (VE). Data are mean±SD. *$P<0.05$ vs YNL. In D, Ea increases ($P<0.0001$) with increases in systemic vascular resistance (SVR) but is higher in OHT at any SVR. In E, aortic elastic modulus (Ao EM$_P$) increases ($P<0.0001$) with increases in MAP, but is higher in OHT at any MAP. In F, systemic arterial compliance (SAC) decreases ($P<0.0001$) with increases in MAP but is lower in OHT at any MAP. The regression model equations are provided in the online supplemental materials.

radioimmunoassay and normalized per mg protein as previously described.[17] LV concentration of TGF-β1 was measured using ELISA and by Western blots. Finally, stored LV tissue samples were processed and loaded onto a 2% SDS-polyacrylamide gel to identify titin isoforms N2B and N2BA[25] and the percent of the more compliant N2BA isoform was determined.

Statistical Analysis

Data are reported as mean±SD. A probability value <0.05 was considered statistically significant. The Student *t* test (2 sided, unpaired) was used to compare groups if the distribution of data met a test for normality (Dallal Kolmogrorov-Smirnov test). As tests for normality in the presence of small numbers of subjects cannot

guarantee a normal distribution, if data met the criteria for normality but still appeared skewed, log transformation was performed before analysis of data to enhance the normality of the distribution. Multiple linear regression was performed to assess the relationship between load and ventricular or vascular properties while adjusting for potential differences between OHT and YNL dogs.

Results

Renal wrapping produced chronic hypertension of a severity similar to that described in a separate group of elderly dogs studied previously.[16] Conscious BP (systolic/diastolic) measured 7 weeks after renal wrapping was 222±23/
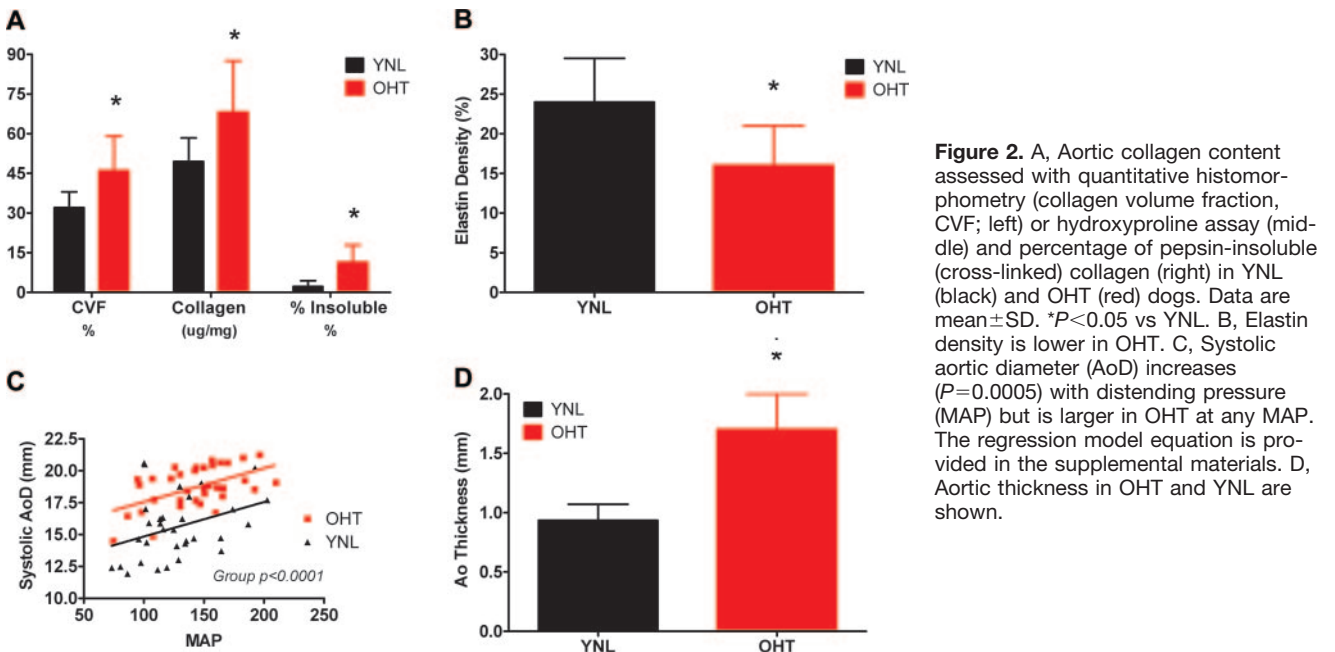
Figure 2. A, Aortic collagen content assessed with quantitative histomorphometry (collagen volume fraction, CVF; left) or hydroxyproline assay (middle) and percentage of pepsin-insoluble (cross-linked) collagen (right) in YNL (black) and OHT (red) dogs. Data are mean±SD. *$P<0.05$ vs YNL. B, Elastin density is lower in OHT. C, Systolic aortic diameter (AoD) increases ($P=0.0005$) with distending pressure (MAP) but is larger in OHT at any MAP. The regression model equation is provided in the supplemental materials. D, Aortic thickness in OHT and YNL are shown.
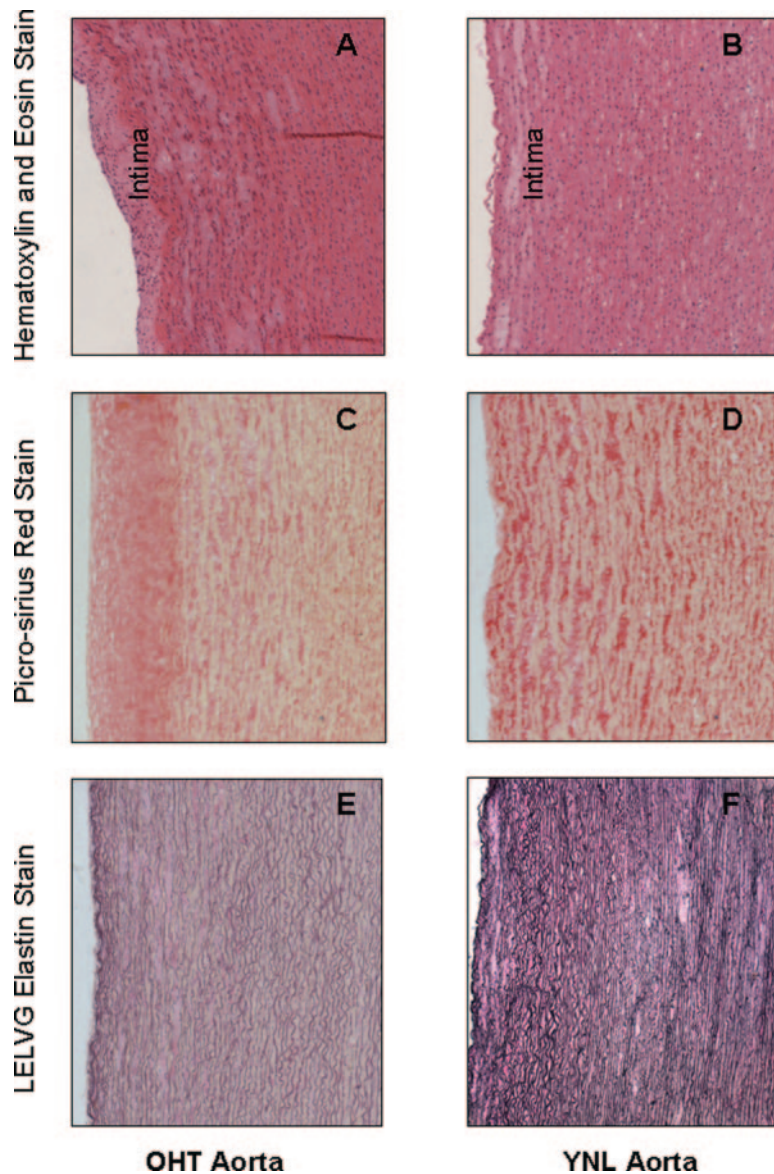
Figure 3. Representative aortic-stained slides from OHT (left) and YNL (right) dogs. Hematoxylin and eosin (A and B) staining shows increased intimal cellularity in OHT dogs. Picros-sirius red (C and D) staining shows increased collagen, particularly in the intima in OHT dogs. LELVG-elastin staining (E and F) shows decreased elastin density with fractured and disrupted elastin fibers in OHT dogs.

135±22 mm Hg in OHT. In a previous study, young normal dogs were instrumented for conscious BP measurement and systolic BP averaged 124.2±9.3 mm Hg.[17]

Vascular Function
During hemodynamic study under anesthesia, systolic and mean aortic pressures as well as Ea were higher or tended to be higher in OHT than YNL except at the PE-2 period (Figure 1A through 1C). For any total load (Ea), SVR was lower in OHT than YNL (Figure 1D). Aortic stiffness as assessed by the elastic modulus increased with increasing distending pressure in both groups but was higher in OHT dogs at any given distending pressure (Figure 1E). Similarly, SAC decreased with increasing MAP in both groups but was lower at any distending pressure in OHT dogs (Figure 1F).

Aortic Structure
Aortic fibrosis as assessed by quantitative histomorphometry and hydroxyproline assay was increased in OHT, as was the amount of collagen cross-linking as reflected by more pepsin-insoluble collagen (Figures 2A and 3A through 3D). Conversely, elastin density (Figures 2B, 3E, and 3F) was lower in OHT, with aortic elastin fibers appearing more fractured and disrupted. Aortic systolic dimension increased with distending pressure but was greater in OHT than YNL at any given pressure (Figure 2C). Aortic wall thickness (Figure 2D) was higher in OHT than YNL.

Baseline LV Function and Hemodynamics
At BL, LV systolic pressure and heart rate were higher; LV diastolic volume was lower in OHT than YNL whereas end-diastolic LV pressure, ejection fraction, and cardiac output were similar between groups (Table). Ees tended to be higher ($P=0.06$) whereas ESV_{200} was lower in the OHT group. The mean values for the diastolic stiffness coefficient (β) and curve fitting constant (α) were similar between groups, however both varied widely within each group with an inverse relationship between β and α (ln α) (see below) and EDV_{20} was lower in OHT than YNL.

Left Ventricular Function and Structure

Parameter	OHT	YNL	P
LV function			
Peak LV systolic pressure, mm Hg	142±18	124±10	0.03
LV end-diastolic pressure, mm Hg	10.6±4.3	8.6±3.5	0.36
Heart rate, bpm	107±11	85±3	0.0004
LV end-diastolic volume, mL	35±9	44±5	0.04
Ejection fraction	0.56±0.13	0.52±0.06	0.52
Cardiac output, L/min	2.04±0.26	1.97±0.37	0.67
E_{es}, mm Hg per mL	7.18±4.38	3.14±2.38	0.06
V_0, mL	−6±6	−33±26	0.04
ESV_{200}, mL	29±14	58±19	0.008
Normalized E_{es}, mm Hg	234±107	132±85	0.07
β, mm Hg/mL	0.076±0.034	0.070±0.045	0.79
α	1.607±1.645	1.051±0.988	0.46
EDV_{20}, mL	45±11	58±9	0.03
LV structure			
LV mass, g/kg body wt	5.33±0.54	4.66±0.43	0.056
ANP, pg/mg protein	5.93±2.04	2.61±0.92	0.009
BNP, pg/mg protein	1.59±1.28	0.56±0.19	0.03
Collagen volume fraction, %	8.3±2.1	4.6±2.0	0.01
LV collagen, μg/mg	2.6±0.7	1.9±0.4	0.007
Insoluble collagen, %	52.4±2.9	45.7±4.9	0.006
Angiotensin II, pg/mg protein	0.076±0.046	0.054±0.024	0.35
TGF-β1, Western	0.47±0.13	0.51±0.10	0.47
Log TGF-β1, ELISA, pg/mL	2.38±0.27	2.66±0.48	0.15
Endothelin, pg/mg protein	0.677±0.222	0.094±0.042	0.02

α indicates curve fitting constant; ANP, atrial natriuretic peptide; β, LV stiffness constant; BNP, brain natriuretic peptide; E_{es}, end-systolic elastance; EDV_{20}, end-diastolic volume at end-diastolic pressure of 20 mm Hg; ESV_{200}, end-systolic volume at end-systolic pressure of 200 mm Hg; TGF-β1, transforming growth factor; V_o, slope-intercept of end-systolic elastance. Data are mean±SD. LV hemodynamic data reflect measurements at baseline before load changes.

The difference in diastolic properties between groups at baseline is illustrated by examples of EDPVR in 2 YNL and 2 OHT dogs in Figure 4. The 3 consecutive IVC occlusions in each dog were highly reproducible. The EDPVR is clearly steeper and shifted leftward/upward in the OHT dogs in both examples; however, in Figure 4A, the β is identical in the 2 dogs, and in Figure 4B, the β is higher in the OHT dog, but the α is higher in the YNL dog. One cannot compare β or α as a single measure of the EDPVR shape and position as they covary in a nonlinear fashion (Figure 4C) which needs to be log transformed (Figure 4D) to be linear. The EDV_{20} parameter accounts for the covariance and its nonlinear nature in a single number to accurately reflect the difference in the EDPVR in the 2 groups.

Relation of LV Systolic and Diastolic Function to Load

Systolic capacitance (ESV_{200}) decreased with increasing Ea in both YNL and OHT. However, the relationship between ESV_{200} and load was shifted in OHT (Figure 5A) toward lower ESV_{200} at any given Ea. Similarly, diastolic capaci-tance (EDV_{20}) decreased with increasing Ea (Figure 5B) in both OHT and YNL dogs. However, EDV_{20} was lower in OHT after adjusting for differences in Ea. The time required for complete LV relaxation as a fraction of diastole also varied with load (ESP) but was greater in OHT after adjusting for differences in ESP (Figure 5C). Findings were similar whether τ was calculated assuming a zero or nonzero asymptote (data not shown). Findings regarding the association of systolic and diastolic stiffness with vascular stiffness and group were similar when lower "common pressures" were used to calculate systolic and diastolic capacitance (ie, ESV_{150} or ESV_{100} and EDV_{10}; data not shown). Further, ESV_{200} and EDV_{20} overlapped well with measured steady-state ESV and EDV when steady-state systolic and diastolic pressures were elevated with phenylephrine (data not shown).

Acute changes in the ESPVR and EDPVR with changes in load in an OHT dog are shown in Figure 6. The average within dog variance (SD of the 3 measurements/average of the 3 measurements, expressed as a percent) for the 3 IVC occlusions performed at each period was 4.1% for EDV_{20} and 7.0% for ESV_{200}.
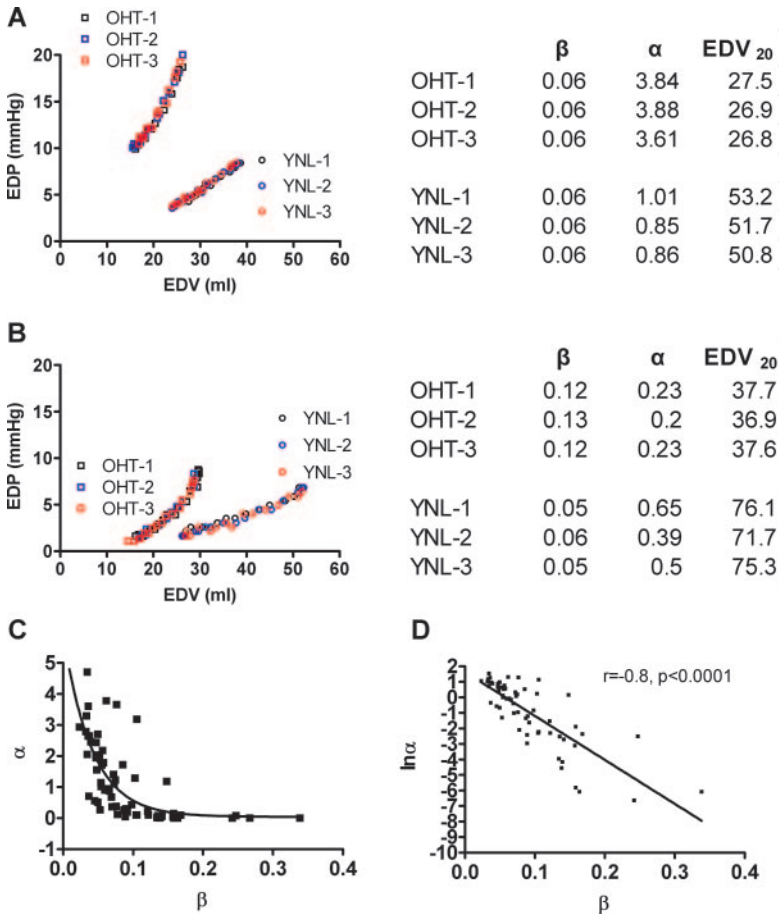
Figure 4. EDPVR in OHT and YNL dogs at baseline: Effect of covariance between the stiffness coefficient (β) and curve fitting coefficient (α). See text for discussion.

LV Structure

LV weight tended to be ($P=0.056$) and LV, ANP, and BNP tissue concentrations (reliable biochemical markers of hypertrophy) were higher in OHT dogs (Table). LV collagen content measured by both methods was higher in OHT, and there was more collagen cross-linking in OHT dogs. OHT dogs had higher tissue levels of ET-1 but similar angiotensin II and TGF-β1 levels. There was no evidence of alterations in titin isoforms in the OHT (% of more compliant N2BA isoform=41.6±4.9%) as compared with YNL (%N2BA= 40.9±8.6%; $P=0.7$). However, as aging itself may cause shifts in titin isoforms, we also analyzed titin isoforms in stored tissue obtained from a separate group of old but nonhypertensive dogs previously studied.[16] The % of the more compliant N2BA isoform was significantly less in the OHT dogs when compared with that observed in age matched nonhypertensive dogs (46.2±4.2%, $P=0.02$), suggesting the potential for the hypertension to have reduced the expression of the more compliant titin isoform in the elderly dogs.

Discussion

Elderly dogs with chronic experimental hypertension displayed increases in arterial load associated with vascular remodeling similar to that described in elderly hypertensive humans, with increased aortic stiffness and decreased systemic arterial compliance, even after adjusting for differences in distending pressure. In both YNL and OHT, acute changes in load were associated with inverse changes in systolic capacitance as previously described.[9–13,16] However, acute changes in load were also associated with inverse changes in diastolic capacitance, which could not be ascribed to relaxation or external forces, suggesting transient load-induced changes in myocardial diastolic stiffness or distensibility. Additionally, adjusting for differences in load between groups, OHT had lower systolic and diastolic capacitance associated with chronic ventricular remodeling and myocardial ET activation.

Age- and Hypertension-Related Vascular Stiffening

As previously reviewed, increases in arterial stiffness with age and hypertension have been reported in multiple studies using a variety of indices reflective of arterial stiffness and its sequela—namely, increases in the speed and magnitude of reflected waves which amplify late systolic pressure and, thus, load on the LV.[2,21] Here we observed striking vascular structural and functional changes and demonstrate that the abnormalities observed in OHT are independent of distending pressure.

The clinical implications of these findings are that regardless of the level of systemic vasoconstriction, Ea will be greater in elderly hypertensives because of the increased arterial stiffness and decreased arterial compliance. Decreases in aortic distensibility have been reported to correlate with exercise intolerance in HFnlEF.[26] The current findings underscore the interaction between increases in vascular stiffness and changes in resistance vessel tone, which may be mediated by abnormalities of endothelial function, baroreflex control,
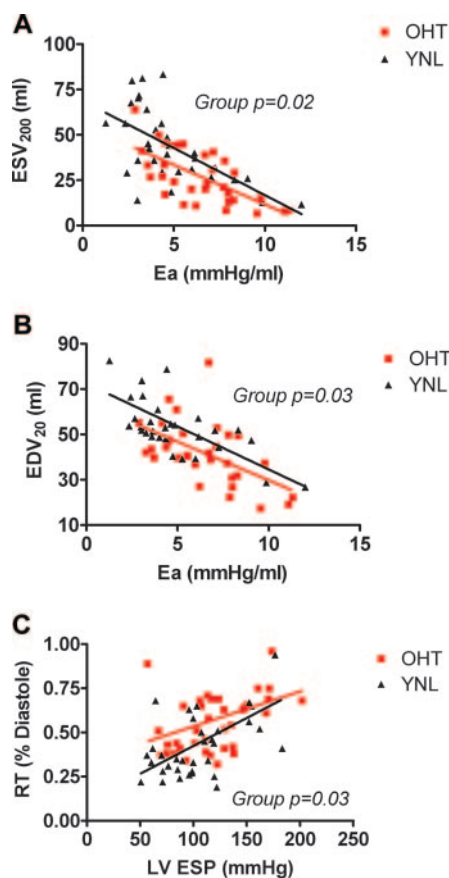
Figure 5. Load dependence of systolic and diastolic function. OHT data in red, YNL data in black. A, Systolic capacitance (ESV_{200}) decreases (↑ contractility, $P<0.0001$) with increases in afterload (effective arterial elastance, Ea) but is lower (↑ contractility) in OHT at any Ea. B, Diastolic capacitance (EDV_{20}) decreases (↑ stiffness, $P<0.0001$) with increases in Ea but is lower (↑ stiffness) in OHT at any Ea. C, Relaxation time (R), represented as a percentage of diastole, increases ($P<0.0001$) with increases in LV end-systolic pressure (LV ESP) but is higher (more prolonged relaxation) at any LV ESP. The regression model equation is provided in the supplemental materials.

or humoral factors and predispose to greater increases in LV load. Of note, systemic vasodilatation with exercise has been reported to be impaired in some but not all studies of HFnlEF.[27,28]

Chronic Ventricular Arterial Coupling

Chronic increases in Ea were coupled to chronic increases in LV systolic stiffness. However, chronic coupling of vascular

and LV diastolic as well as systolic stiffness in humans is well described,[29,30] and similar to our previous series,[16] at baseline, the diastolic stiffness constant was not increased in the OHT dogs. We had speculated that the lack of increase in β could be attributable to covariance between the stiffness constant β and the curve fitting constant α which can limit the ability to characterize the EDPVR shape and position with a single parameter. In this series, controlling for this covariance by calculating diastolic capacitance revealed differences in the EDPVR between groups. Although increases in diastolic stiffness will often be evident from increases in β, this is not always the case, and the importance of using proper methods to compare the EDPVR between groups has been recently and comprehensively reviewed[18] and is further illustrated here in Figure 4.

Acute Ventricular Arterial Coupling

The potential for enhanced contractility to result in shifts in the position or slope of the ESPVR as measured in vivo has been previously reviewed.[18] Indeed, previous studies in anesthetized and conscious normal dogs have demonstrated that the slope of the ESPVR is increased or the ESPVR is shifted leftward with acute increases in Ea such that SW is maximized in the absence of increases in EDV.[9–13] The effect of increases in the slope or shifts in the position is captured by calculation of systolic capacitance (ESV_{200}). The capacity for afterload enhancement of myocardial performance is lost in animal models of systolic dysfunction[31] but preserved in this model which combines features of aging and chronic pressure overload.[16] Previous studies suggest that these shifts are independent of the mode (vasoconstrictor infusion or aortic occlusion) used to increase Ea, autonomic blockade, or the presence of anesthesia.[9–13]

Whereas the effect of afterload on systolic performance has been studied, there are very few studies regarding the effect of afterload on the EDPVR. An elegant study in humans with variable types of cardiovascular disease using single beat assessment of holo-diastolic PVR reported that increases in afterload (angiotensin infusion) shifted the entire holo-diastolic PVR upward.[14] Whereas the investigators speculated that this was mediated by the right ventricle or pericardium (external forces), we show that the entire EDPVR described with acute preload reduction to release external forces was shifted upward with increases in Ea. As time for complete relaxation rarely extended past 80% of diastole, this effect cannot be explained by prolonged relaxation affecting end-
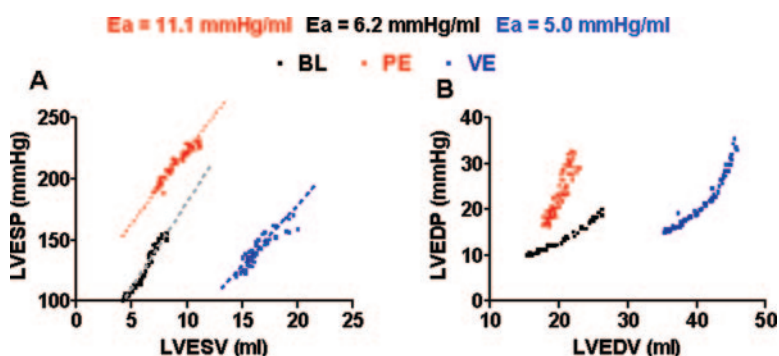
Figure 6. Representative example of the ESPVR (left) and EDPVR (right) at baseline (black), phenylephrine administration (PE-2, red), and volume expansion (blue) in an OHT dog.

diastolic pressures defined during preload reduction. However, load-mediated impairment in relaxation could impinge on diastolic PVR if associated with tachycardia.[20] Of note, in the study of Ghandi et al, heart rates were actually lower during rather than after hypertensive pulmonary edema and averaged <80 bpm at both time points.[6] The association between load and systolic and diastolic capacitances was evident in both YNL and OHT dogs, suggesting that this is a fundamental feature of LV function not restricted to disease states. The current findings are also consistent with a recent study describing diastolic VA coupling based on analysis of pressure phase plane-derived indices in humans.[32]

Mechanisms of Load Dependency

This study cannot definitively elucidate the mechanisms responsible for chronic or acute systolic and diastolic VA coupling. The geometric changes, hypertrophy, extracellular matrix changes, and myocardial activation of ET,[33] may contribute to chronic increases in systolic and diastolic stiffness. Interestingly, we did not detect differences in LV TGF-β1 or angiotensin II despite the presence of increased LV fibrosis in OHT dogs. Whereas these humoral factors are important mediators of myocardial collagen synthesis, their activation may be transient.[34,35] Although differences in titin isoform distribution between YNL and OHT dogs were not evident, location of myocardial sampling for the titin assays was not standardized; this may interfere with the ability to demonstrate differences. Decreases in the relative abundance of the more compliant N2BA titin isoform have been demonstrated in humans with HFnlEF.[36] Additionally, variable and species-specific changes in titin isoform composition have been described in the fetal to adult transition, but changes with aging have not been explored.[37] Thus, the very preliminary differences observed in the age-matched nonhypertensive dogs are of note but must be confirmed in future studies with more appropriate control of sampling location.

The mechanisms responsible for acute coupling of load and myocardial systolic performance have been previously reviewed.[18] Bronzwaer and Paulus have made a cogent argument for residual diastolic myofilamentary interaction in mediating decreases in distensibility with acute increases in afterload in hypertrophied myocardium that is relevant to the current observations.[15] Certainly, the concept of "passive" diastolic stiffness is increasingly irrelevant as dynamic changes in energetics and other factors affecting phosphorylation status of titin and regulatory proteins modifying calcium handling or sensitivity may alter myocardial diastolic stiffness or distensibility acutely.[15,38] Similarly, it appears that dynamic changes in systolic and diastolic properties in addition to chronic resting diastolic dysfunction may mediate hemodynamics and symptoms in some patients with HFnlEF.[5,27,39]

Limitations

Studies were performed under anesthesia and autonomic blockade, and restoration of blood pressure to conscious levels with vasopressor infusion may not recapitulate all features observed in the conscious state. Future studies that investigate hemodynamics in a conscious animal model of hypertensive heart disease would be helpful to confirm this data. We did not measure right ventricular volume and pressure but used preload reduction to avoid effects of ventricular interdependence and pericardial constraint. As infusion of dextran could affect parallel conductance, we did recalibrate completely before measurements after volume expansion. No animal model can faithfully recapitulate all the features known or postulated to be important to the pathophysiology of HFnlEF including the potential evolution of ventricular or vascular changes over a longer duration of hypertension.[40]

Perspectives

In this elderly hypertensive canine model, chronic changes in vascular and ventricular stiffness predispose to, and interact with, fluctuations in blood pressure producing load-dependent decreases in systolic and diastolic LV capacitance and impairment in relaxation kinetics. These findings have relevance to the pathogenesis of HFnlEF in elderly patients with hypertensive heart disease.

Disclosures

None.

References

1. Owan TE, Redfield MM. Epidemiology of diastolic heart failure. *Prog Cardiovasc Dis*. 2005;47:320–332.
2. Zieman SJ, Melenovsky V, Kass DA. Mechanisms, pathophysiology, and therapy of arterial stiffness. *Arterioscler Thromb Vasc Biol*. 2005;25:932–943.
3. Frenneaux M, Williams L. Ventricular-arterial and ventricular-ventricular interactions and their relevance to diastolic filling. *Prog Cardiovasc Dis*. 2007;49:252–262.
4. Kass DA. Ventricular arterial stiffening: integrating the pathophysiology. *Hypertension*. 2005;46:185–193.
5. Kawaguchi M, Hay I, Fetics B, Kass DA. Combined ventricular systolic and arterial stiffening in patients with heart failure and preserved ejection fraction: implications for systolic and diastolic reserve limitations. *Circulation*. 2003;107:714–720.
6. Gandhi SK, Powers JC, Nomeir AM, Fowle K, Kitzman DW, Rankin KM, Little WC. The pathogenesis of acute pulmonary edema associated with hypertension. *N Engl J Med*. 2001;344:17–22.
7. Warner JG Jr, Metzger DC, Kitzman DW, Wesley DJ, Little WC. Losartan improves exercise tolerance in patients with diastolic dysfunction and a hypertensive response to exercise. *J Am Coll Card*. 1999;33:1567–1572.
8. Cuocolo A, Sax FL, Brush JE, Maron BJ, Bacharach SL, Bonow RO. Left ventricular hypertrophy and impaired diastolic filling in essential hypertension. Diastolic mechanisms for systolic dysfunction during exercise. *Circulation*. 1990;81:978–986.
9. Schipper IB, Steendijk P, Klautz RJ, van der Velde ET, Baan J. Cardiac sympathetic denervation does not change the load dependence of the left ventricular end-systolic pressure/volume relationship in dogs. *Pflugers Arch*. 1993;425:426–433.
10. van der Linden LP, van der Velde ET, van Houwelingen HC, Bruschke AV, Baan J. Determinants of end-systolic pressure during different load alterations in the in situ left ventricle. *Am J Physiol*. 1994;267:H1895–H906.
11. Little WC, Cheng C-P. Left ventricular-arterial coupling in conscious dogs. *Am J Physiol Heart Circ Physiol*. 1991;261:H70–H76.
12. van der Velde ET, Burkhoff D, Steendijk P, Karsdon J, Sagawa K, Baan J. Nonlinearity and load sensitivity of end-systolic pressure-volume relation of canine left ventricle in vivo. *Circulation*. 1991;83:315–327.

13. Freeman GL, Little WC, O'Rourke RA. The effect of vasoactive agents on the left ventricular end-systolic pressure-volume relation in closed-chest dogs. _Circulation_. 1986;74:1107–1113.

14. Alderman EL, Glantz SA. Acute hemodynamic interventions shift the diastolic pressure-volume curve in man. _Circulation_. 1976;54:662–671.

15. Bronzwaer JG, Paulus WJ. Matrix, cytoskeleton, or myofilaments: which one to blame for diastolic left ventricular dysfunction? _Prog Cardiovasc Dis_. 2005;47:276–284.

16. Munagala VK, Hart CY, Burnett JC Jr, Meyer DM, Redfield MM. Ventricular structure and function in aged dogs with renal hypertension: a model of experimental diastolic heart failure. _Circulation_. 2005;111: 1128–1135.

17. Hart CY, Meyer DM, Tazelaar HD, Grande JP, Burnett JC Jr, Housmans PR, Redfield MM. Load versus humoral activation in the genesis of early hypertensive heart disease. _Circulation_. 2001;104:215–220.

18. Burkhoff D, Mirsky I, Suga H. Assessment of systolic and diastolic ventricular properties via pressure-volume analysis: a guide for clinical, translational, and basic researchers. _Am J Physiol Heart Circ Physiol_. 2005;289:H501–H512.

19. Zile MR, Baicu CF, Gaasch WH. Diastolic heart failure–abnormalities in active relaxation and passive stiffness of the left ventricle. _N Engl J Med_. 2004;350:1953–1959.

20. Hay I, Rich J, Ferber P, Burkhoff D, Maurer MS. Role of impaired myocardial relaxation in the production of elevated left ventricular filling pressure. _Am J Physiol Heart Circ Physiol_. 2005;288:H1203–H1208.

21. Nichols WW, O'Rourke M. _McDonald's Blood Flow in Arteries_. Third ed. Philadelphia, PA: Lea & Febiger; 1990.

22. Peterson L, Jensen R, Parnell J. Mechanical properties of arteries in vivo. _Circulation_. 1960;8:622–639.

23. Liu Z, Brin KP, Yin FC. Estimation of total arterial compliance: an improved method and evaluation of current methods. _Am J Physiol_. 1986;251:H588–H600.

24. Stegemann H, Stalder K. Determination of hydroxyproline. _Clin Chim Acta_. 1967;18:267–273.

25. Makarenko I, Opitz CA, Leake MC, Neagoe C, Kulke M, Gwathmey JK, del Monte F, Hajjar RJ, Linke WA. Passive stiffness changes caused by upregulation of compliant titin isoforms in human dilated cardiomyopathy hearts. _Circ Res_. 2004;95:708–716.

26. Hundley WG, Kitzman DW, Morgan TM, Hamilton CA, Darty SN, Stewart KP, Herrington DM, Link KM, Little WC. Cardiac cycle-dependent changes in aortic area and distensibility are reduced in older patients with isolated diastolic heart failure and correlate with exercise intolerance. _J Am Coll Cardiol_. 2001;38:796–802.

27. Borlaug BA, Melenovsky V, Russell SD, Kessler K, Pacak K, Becker LC, Kass DA. Impaired chronotropic and vasodilator reserves limit exercise capacity in patients with heart failure and a preserved ejection fraction. _Circulation_. 2006;114:2138–2147.

28. Hundley WG, Bayram E, Hamilton CA, Hamilton EA, Morgan TM, Darty SN, Stewart KP, Link KM, Herrington DM, Kitzman DW. Leg flow-mediated arterial dilation in elderly patients with heart failure and normal left ventricular ejection fraction. _Am J Physiol Heart Circ Physiol_. 2007;292:H1427–H1434.

29. Chen CH, Nakayama M, Nevo E, Fetics BJ, Maughan WL, Kass DA. Coupled systolic-ventricular and vascular stiffening with age: implications for pressure regulation and cardiac reserve in the elderly. _J Am Coll Cardiol_. 1998;32:1221–1227.

30. Redfield MM, Jacobsen SJ, Borlaug BA, Rodeheffer RJ, Kass DA. Age- and gender-related ventricular-vascular stiffening: a community-based study. _Circulation_. 2005;112:2254–2262.

31. Prabhu SD, Freeman GL. Altered LV inotropic reserve and mechanoenergetics early in the development of heart failure. _Am J Physiol Heart Circ Physiol_. 2000;278:H698–H705.

32. Chung CS, Strunc A, Oliver R, Kovacs SJ. Diastolic ventricular-vascular stiffness and relaxation relation: elucidation of coupling via pressure phase plane-derived indexes. _Am J Physiol Heart Circ Physiol_. 2006;291: H2415–H2423.

33. Yamamoto K, Masuyama T, Sakata Y, Nishikawa N, Mano T, Hori M. Prevention of diastolic heart failure by endothelin type A receptor antagonist through inhibition of ventricular structural remodeling in hypertensive heart. _J Hypertens_. 2002;20:753–761.

34. Kuwahara F, Kai H, Tokuda K, Kai M, Takeshita A, Egashira K, Imaizumi T. Transforming growth factor-beta function blocking prevents myocardial fibrosis and diastolic dysfunction in pressure-overloaded rats. _Circulation_. 2002;106:130–135.

35. Villacorta H, Dillmann W. Cardiac hypertrophy-induced changes in mRNA levels for TGF-B1, fibronectin, and collagen. _Am J Physiol Heart Circ Physiol_. 1992;262:H1861–H1866.

36. van Heerebeek L, Borbely A, Niessen HW, Bronzwaer JG, van der Velden J, Stienen GJ, Linke WA, Laarman GJ, Paulus WJ. Myocardial structure and function differ in systolic and diastolic heart failure. _Circulation_. 2006;113:1966–1973.

37. Kruger M, Kohl T, Linke WA. Developmental changes in passive stiffness and myofilament Ca^{2+} sensitivity due to titin and troponin-I isoform switching are not critically triggered by birth. _Am J Physiol Heart Circ Physiol_. 2006;291:H496–H506.

38. Kass DA, Bronzwaer JG, Paulus WJ. What mechanisms underlie diastolic dysfunction in heart failure? _Circ Res_. 2004;94:1533–1542.

39. Brubaker PH, Marburger CT, Morgan TM, Fray B, Kitzman DW. Exercise responses of elderly patients with diastolic versus systolic heart failure. _Med Sci Sports Exerc_. 2003;35:1477–1485.

40. Klotz S, Hay I, Zhang G, Maurer M, Wang J, Burkhoff D. Development of heart failure in chronic hypertensive Dahl rats: focus on heart failure with preserved ejection fraction. _Hypertension_. 2006;47:901–911.

Acute and Chronic Ventricular-Arterial Coupling in Systole and Diastole: Insights From an Elderly Hypertensive Model

Brian P. Shapiro, Carolyn S.P. Lam, Jeetendra B. Patel, Selma F. Mohammed, Martina Kruger,
Donna M. Meyer, Wolfgang A. Linke and Margaret M. Redfield

The online version of this article, along with updated information and services, is located on the
World Wide Web at:
http://hyper.ahajournals.org/content/50/3/503

Data Supplement (unedited) at:
http://hyper.ahajournals.org/content/suppl/2007/06/18/HYPERTENSIONAHA.107.090092.DC2

Online Data Supplement:

Methods:

General methods:

Prior to entry into this study, all dogs underwent an evaluation by a research veterinarian including physical examination, echocardiography, electrolytes, liver function tests, and renal function tests to exclude co-morbidities. Creatinine did not change after renal wrapping in the OHT group (Week 0, 0.75±0.2mg/dl; Week 8, 0.80±0.24mg/dl, p=ns). There was no echocardiographic, electrocardiographic or gross pathological evidence of myocardial ischemia or infarction before or during the acute study.

Acute Hemodynamic Study

During the acute study, normal saline (3 ml/min) was infused to replace insensible losses. The micromanometer catheter was obtained from Millar Instruments, Houston, TX. The aortic volumetric flow probe was obtained from Transonics, Ithaca, NY. Aortic piezoelectric crystals were obtained from Sonometrics, Ontario, Canada. The LV conductance catheter was obtained from Leycom, Holland or Millar Instruments, Houston, TX. The pneumatic inferior vena cava (IVC) occluder was obtained from In Vivo Metric, Healdsburg, California. The pericardium remained intact. All transducers were calibrated against a standard strain gauge transducer. The delay in aortic flow probe signal of eight ms was corrected for in subsequent analysis. All data were collected at end-expiration with ventilation briefly suspended. Harvested tissue samples were stored in formalin or flash-frozen in liquid nitrogen and stored at -80°C.

Hemodynamic Analysis

Data were acquired at 250 Hz and analyzed using customized commercially available software (Sonometrics, Ontario, Canada). End-diastole was defined by the ECG whereas end-systole was the top left corner of the pressure-volume loop. The diastolic period was calculated as: RR interval – the duration from end-diastole to end-systole (as defined above).

Histological and Biochemical Analysis

Aortic wall thickness was measured from the internal to external elastic laminae from formalin-fixed aortic sections and averaged from five locations spanning the circumference of the aorta. Quantitative histomorphometric measurements utilized a commercially available image processing system (Zeiss Vision, Germany).

The transforming growth factor-β1 (TGF-β1) ELISA kit was obtained from R&D Systems, Minneapolis, MN. The SDS-gel electrophoresis TGF-β1 polyclonal rabbit antibody was obtained from Santa Cruz, California. Signals were normalized to the actin signal using ImageJ software, Bethesda, Maryland.

Figures:

The linear regression equations giving the model fits and parameter estimates for the variables included in the models are shown here:

Figure 1.

Panel D: Ea=0.08+0.001*SVR+0.67 if OHT; Model r=0.95, p<0.0001
SVR p<0.0001, Group p<0.0001

Panel E: $AoEM_P * 10^6$=-0.132+(0.007*MAP)+0.129 if OHT: Model r = 0.67, p < 0.0001
MAP p<0.0001, Group p=0.004

Panel F: SAC =0.6157-(0.0025*MAP)-0.0587 if OHT; Model r = 0.62, p < 0.0001
MAP p<0.0001, Group p=0.0015

Figure 2.

Panel C: AoD =13.5+(0.027*MAP)+1.35 if OHT; Model r= 0.69, p < 0.0001
MAP p=0.0005, Group p<0.0001

Figure 5.

Panel A: ESV_{200}=62.5-4.8*Ea-4.3if OHT; Model r=0.71, p<0.0001
Ea p<0.0001, Group p=0.02

Panel B: EDV_{20}=68.4-3.6*Ea-3.2 if OHT; Model r=0.69, p<0.0001
Ea p<0.0001, Group p=0.03

Panel C: RT=0.22+0.0026*ESP+0.05if OHT: Model r=0.53, p<0.0001
ESP p<0.0001, Group p=0.03